Segmented Hairpin Topology for Reduced Losses at High Frequency Operations

Eraldo Preci, Stefano Nuzzo, Member, IEEE, Giorgio Valente, David Gerada, Member, IEEE, Davide Barater, Member, IEEE , Michele Degano, Member, IEEE ,Giampaolo Buticchi, Senior Member, IEEE, Chris Gerada, Senior Member, IEEE

Abstract – **Nowadays, one of the key challenges in transport electrification is the reduction of components' size and weight. The electrical machine plays a relevant role in this regard. Designing machines with higher rotational speeds and excitation frequencies is one of the most effective solutions to increase power densities, but this comes at the cost of increased losses in cores and windings. This challenge is even more pronounced in preformed windings, such as hairpins, which enable higher slot fill factors and shorten manufacturing cycle times. In this work an improved hairpin winding concept is proposed, aiming to minimize high-frequency losses while maintaining the benefits deriving from the implementation of hairpin windings onto electrical machines. Analytical and finite element models are first used to assess the high-frequency losses in the proposed winding concept, namely the segmented hairpin, proving the benefits compared to conventional layouts. Experimental tests are also performed on a number of motorettes comprising both conventional and proposed segmented hairpin configurations. Finally, these experimental results are compared against those collected from motorettes equipped with random windings, demonstrating the competitiveness of the segmented hairpin layout even at high-frequency operations.**

***Index Terms*— AC losses, high frequency, automotive, electrical machine, winding, hairpin winding, segmented hairpin, random, end winding, analytic model, experimental, mass production..**

I. INTRODUCTION

Nowadays, transport electrification is one of the most viable solutions to reduce emissions and meet fuel economy requirements. Hybrid and pure electric vehicles are being developed for all transport applications [1],[2],[3],[4]. Besides these requirements, power density, efficiency and reliability are also objectives of primary importance to achieve when designing a more electric vehicle. In this regard, the components of the vehicle's powertrain play a key role. Of these, the electrical machine is experiencing an ever-increasing interest and research focusing on the maximization of their power density [5], efficiency [6] and reliability [7] is now underway at an unprecedented rate.

Nevertheless, achieving all these requirements concurrently is a difficult task. In fact, while the operating speed represents the main lever to increase the machine power for a given volume [8], it results in higher operating frequencies. These, in turn, reflect on increased losses in cores and windings as well as higher stresses on coil insulations, thus efficiency and reliability are compromised [9],[10]. An evident example in this regard is represented by hairpin windings, whose full penetration in the transportation market is curbed by their inherently high ohmic losses at high frequency operations, where skin and proximity effects occur.

On the other hand, this technology offers higher slot fill factors, reduced end-winding lengths and lower low frequency copper losses than their random-wound counterpart. In addition, their manufacturing allows for automatized, repeatable and reliable procedures, making hairpin windings ideal when high production volumes are required, such as in automotive transportation. In this case, the cost minimization is another key driver. Studies carried out in [11] have proven that, for a production target of 1 million units per year, manufacturing hairpin stators is cheaper than manufacturing stators employing random windings. It becomes then clear why hairpin windings are considered by many scholars and industries as the way forward for next generation electrical machines [12].

However, the bottle-neck remains the ohmic loss produced at high frequency operation (AC losses). Therefore, to fully meet the green revolution requirements, hairpin designs should be aimed to mitigate this challenge. In the last few years, the focus of several researches has been on ways to model, estimate and reduce AC losses in hairpins. In [13], guidelines on how to make suitable connections for reduced losses have been provided, along with a 1D model for the evaluation of copper losses. In [14], a 2D analytical model has been proposed and validated via finite element analysis (FEA). Methods such as removing the closest conductor to the slot opening or reducing the conductors' height while increasing the number of conductors have been proposed to reduce AC losses [15]. However, the first solution reduces the fill factor since part of the slot is left empty [16], whereas the second option increases the manufacturing complexity [13]. Asymmetric windings consisting of series-connected conductors featuring different cross-sections have been studied via FEA in [17]. Here, promising results have been achieved, but an experimental validation is missing. In addition, the method increases the DC resistance of the asymmetric conductors and may represent a limit to the maximum obtainable current density.

E. Preci, G.Valente,M. Degano, D. Gerada, G. Buticchi and C. Gerada are with the Power Electronics, Machines and Control Group, University of Nottingham, Nottingham NG72RD, U.K., and also with the Faculty of Science and Engineering of University of Nottingham NingboChina,Ningbo315100,China.(email:eraldo.preci2@nottingham.edu.cn;ezzmd2@exmail.nottingham.ac.uk;ezzdg2@exmail.nottingham.ac.uk;Giampaolo.Buticchi@nottingham.edu.cn; eezcg@exmail.nottingham.ac.uk)

S. Nuzzo and D. Barater are with Department of Engineering Enzo Ferrari, University of Modena and Reggio Emilia, Modena 41125, Italy. (e-mail: stefano.nuzzo@unimore.it; davide.barater@unimore.it)

Another interesting technique to reduce AC losses in hairpin windings comes from the "strand" concept typical of random windings, where the conductor is divided in several parallel-connected sub-conductors (strands). In hairpins, this method cannot be applied as flexibly as in random windings. The number of parallel-connected elements should be kept low to avoid unfeasible solutions or excessive complications of the bending and welding processes [18]. Although the concept of parallel conductors has been widely implemented in large power machines equipped with pre-formed winding [19], to the of the authors' knowledge the parallel-connected concept in hairpin windings has been proposed in [20] for the first time, but the analysis only focused on the 2D aspects (i.e. end-windings effects are neglected) and no experimental validation was provided.

This work fills these gaps by including the 3D effects in both analytical and FE models and, most importantly, by experimentally validating the segmented hairpin concept. In particular, concerning the modelling aspects, a simplified 2D FE model is proposed for the analysis of the end regions, yet taking into account the phenomena potentially occurring at high frequencies. Regarding the experimental validation, a segmented hairpin winding is implemented onto purposely-built motorettes. Four motorettes are prototyped and tested, each of them equipped with different winding arrangements for comparative analyses. Besides proving the benefits of the proposed technique in terms of loss reduction, the experimental results are used to demonstrate that the segmented hairpin winding can compete against random windings even at high frequency operations. This is done by comparing these results to those obtained in [21] on motorettes equipped with round wire random windings.

II. Background and Proposed Concept

This work considers an electrical machine designed for automotive traction with power and maximum speed equal to 115 kW and 12000 rpm, respectively. As detailed in [20], the design and optimization process of such traction motor has led to select a permanent magnet assisted synchronous reluctance machine with 4 poles and 3 rotor barriers per pole, as shown in Fig 1, and the geometrical parameters are provided in Table I. Regarding the stator, two different numbers of slots-per-pole-per-phase q are envisioned (i.e. q=2 and q=4), while fixing stator inner and outer diameters. Also in [20], both random and hairpin windings have been considered for the designed motor. In this work, the focus is on the hairpin option and the following layouts are considered: 1) q=2 and number of layers per slot k=4; 2) q=4 and k=8; 3) q=4 and k=44) q=4 and k=6. For the sake of completeness, the main stator dimensions are provided in Table II, whereas the conductors' dimensions are given in Table III.

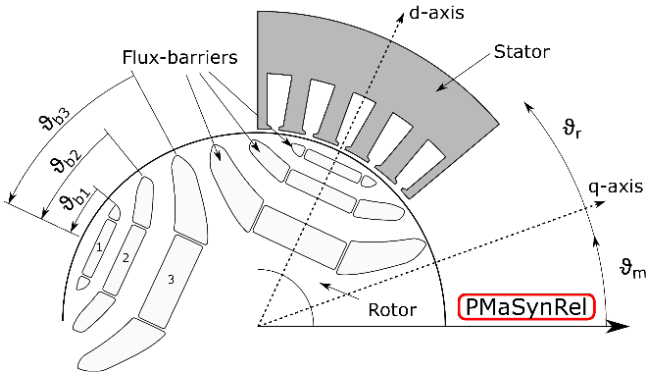

Figure 1: Permanent Magnet assisted SynRel motor sketch [20].

Table I: Motor Geometrical Parameters

Name	Description
ϑ_{b1}	Flux barrier angle 1
ϑ_{b2}	Flux barrier angle 2
ϑ_{b3}	Flux barrier angle 3
W_{so}	Slot opening width
h_s	Slot height
W_{pmi}	Flux Permanent Magnetmagnet width
h_{pmi}	Permanent MagnetFlux magnet height

In reality, layouts 3) and 4) are electrically identical, i.e. the number of equivalent conductors in series per slot is four for both layouts. However, layout 4) implements the proposed segmented hairpin concept, consisting of splitting some of the conductors in two or more layers. This concept can be extended to any hairpin winding configuration (i.e. different number of layers or different parallel paths), and does not impact the equivalent number of turns per phase but only splits one or more conductors in two or more smaller parallel-connected conductors, with the aim of reducing the AC copper losses. To better envisage this concept, in Fig. 2a the conventional solution corresponding to option 3) is modified by segmenting the two closest conductors to the slot opening in two sub-layers having identical cross sections. This modified layout is named "proposed solution" in Fig. 2a and corresponds to the aforementioned option 4), where the number of conductors is series per slot is four, but the number of layers per slot is six. For this reason, this layout can be labelled with "k=4 segmented", as seen in Table III. Thanks to Table III we can note that both solutions have the same fill factor, the segmented layers result placed nearer to the slot opening zone because the physical gap needed between the layers. The electrical connections of the segmented hairpin winding are shown in Fig. 2b, where each of the last two conductors (namely 3 and 4) are subdivided in two sub-layers (3.1 and 3.2, and 4.1 and 4.2), whereas in Fig. 2c the connections typical of a standard hairpin layout are illustrated to highlight the major differences.

Table II: Motorette Geometrical Parameters

Description	Value(mm) q=2	Value(mm) q=4
Stator Inner Radius	70	
Stator Outer Radius	111	
Stack length	92	
Slot width	9.1	4.4
Slot height	23	20

Table III :Bar Cross Section Parameters

Description	Value(mm) Width	Height
Layout 1): q=2, k=4	8.2	4.3
Layout 2): q=4, k=8	4	1.75
Layout 3): q=4, k=4	4	3.5
Layout 4): q=4, k=4 (k=4 segmented)	4	1.75

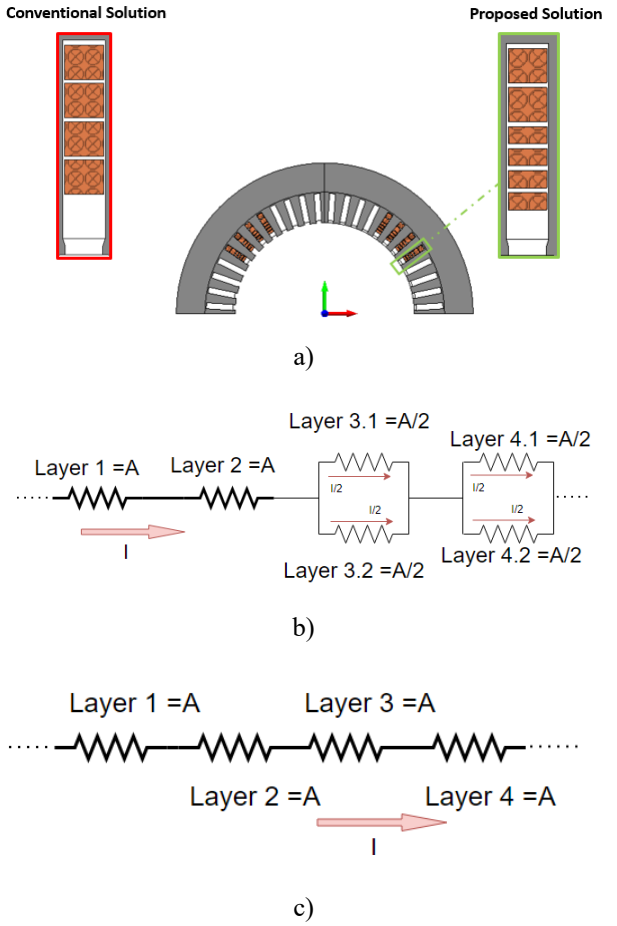

Fig. 2. a) the proposed segmented hairpin concept and b) circuital schematic; c) conventional hairpin circuital schematic

A. Manufacturing considerations

In theory, each segmented conductor can be composed of more than two parallel-connected layers. However, using more than two sub-layers may complicate the manufacturing process, taking into account that 1) a transposition is needed to make the segmented technique effective, 2) the number of welding points increases and 3) the total number of layers per slot increases too. Therefore, in this work, it is deemed sufficient to segment only two conductors. These are obviously the closest to the stator slot openings, being the most critical ones from a loss perspective. Additionally, the number of sub-layers is chosen equal to two, thus minimizing the impact on the manufacturing.

Assuming a high-volume production context, the hairpin manufacturing would be a fully automated process. Thanks to the technology progress in hairpin manufacturing lines, the segmented hairpin winding will not have a significant impact on the manufacturing process and cost. In fact, even if the number of elementary pins to use increases, nowadays several configurable tooling can be used to bend and twist them, and this allows to use the same manufacturing line for all the types of pins. Attention must be paid to the constraints related to the hairpins' width-to-height ratio during the bending process. Additionally, the number of conductors must be kept below the current manufacturing limitation. In other words, as long as the width-to-height ratio and the number of layers per slot are kept below the current limits, then no complications are seen when implementing the segmented technology. Regarding the welding points, if a standard hairpin winding was to be considered for the application at hand, then the number of welding points would have been 15, whereas the proposed segmented layout presents 22 welding points. This does not represent a significant complication. Moreover, the technology progress in manufacturing lines is leading to manage the welding process in a very reliable way, thus avoiding the risk of short circuits in actual applications.

An example of these technology progresses is represented by AUTO-MEA (Automated Manufacturing of wound components for next generation Electrical machines) [22], a Clean Sky 2 project which aims to develop novel methodologies for winding design and to deliver an innovative and flexible coil fabrication system, which can provide programmable 3D formed coil shapes suitable for high frequency operation, effective coil insertion and automated welding strategies to form a complete winding system for aerospace and automotive wound components.
Although a detailed cost-benefit analysis is impossible to carry out if the volume production is not specified, it is anyway clear that the segmentation concept will not bring a significant cost increment to the overall process, while the benefits in terms of loss reduction and energy savings can be impressive. This would lead to a series of additional benefits such as higher efficiencies, lower temperatures, increased insulation lifetimes, etc.

III. Analytical Model

To exploit the benefits of the proposed methodology vs. conventional ones, a 1D analytical model for AC loss estimation is developed and described in this section.

AC losses are those occurring above the frequency level where the current is no longer uniformly distributed within the conductors. These losses are mostly due to skin and proximity effects, assuming that circulating currents are zeroed by a suitable transposition. Usually, the AC losses PAC are quantified through the product of DC losses and a non-dimensional factor KAC, which is defined in (1). The DC loss PDC is found through the simple relationship reported in (2), where lc and Ac are respectively the conductor length and its cross section, while σ is the electric conductivity of the material. When skin and proximity effects occur, the cross section where the current flows is a fraction of Ac, thus the equivalent resistance (namely the AC resistance) increases and AC losses are consequently enhanced by the factor KAC.

$$K_{AC} = \frac{P_{AC}}{P_{DC}} \tag{1}$$

$$P_{DC} = R_{DC} I^2 = \frac{l_c}{\sigma A_c} I^2 \tag{2}$$

These high-frequency phenomena can be significant especially in the slot region, but they may have some

influence also in the end-winding regions. Hence, both regions are modelled analytically aiming to accurately estimate the overall AC losses.

A .Slot Region Model

A 1D model is developed leveraging on the discretization of the domain under investigation. This allows to achieve an acceptable accuracy while minimizing the calculation effort. The slot domain under analysis is shown in Fig. 3 and consists of a single slot comprising k conductors (hairpin legs). This domain can be analyzed using the discretization layer approach, where each conductor is located in a layer. The magnetic field inside the slot produced by the current flowing in the conductors is considered parallel to their width Wck, meaning that the field component parallel to their height hc is neglected.

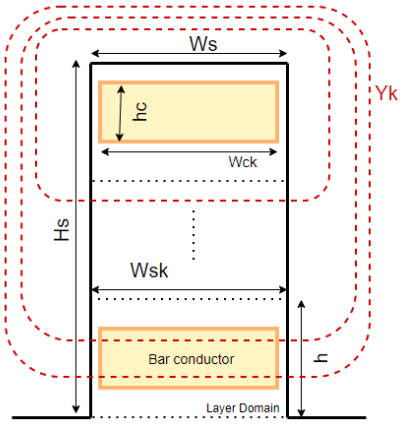

Fig. 3. Discretized domain.

Under the assumptions of linear behavior of the ferromagnetic materials, the application of the Ampere's law to any of the red circuits Yk shown in Fig. 4 leads to obtain (3). Here, H is the magnetic field strength, Wsk is the slot width, Jk is the current density in the k-th layer, yk-1 and yk are the (k-1)-th and k-th layers and Ik-1 is the total current linking the (k-1)-th loop.

$$H\,W_{sk} = \int_{y_{k-1}}^{y_k} -J_k\,W_{ck}\;\;dr + \;I_{k-1} \tag{3}$$

Exploiting (3) leads to the partial differential equations provided in (4) and (5), where the physical quantities can be expressed by phasors thanks to the hypothesis of sinusoidal current feeding the conductors. In (5), ω is the supply electric pulsation, while μ is the magnetic permeability of the conductive material.

$$\frac{\delta H}{\delta r} = \frac{-J_k\,w_{ck}}{w_{sk}} \tag{4}$$

$$\frac{\delta J}{\delta r} = -\,\mu\,\sigma\,\frac{\delta H}{\delta t} = \;-j\,\omega\,\mu\,\sigma\,H \tag{5}$$

Combining (4) and (5) leads to obtain (6), the general solution of which is provided in (7). Here, the quantity η is the skin depth which is defined as in (8).

$$\frac{\delta^2 H}{\delta r^2} - \frac{j\,\omega\,\mu\,\sigma\,H\,W_{ck}}{W_{sk}} = 0 \tag{6}$$

$$H = \;A_1\,e^{-\left(\frac{1+j}{\eta}\right)r} + \;A_2\,e^{\left(\frac{1+j}{\eta}\right)r} \tag{7}$$

$$\eta = \sqrt{\frac{W_{sk}\;2}{W_{ck}\;\omega\;\mu\;\sigma}} \tag{8}$$

The constant terms A1 and A2 involved in (7) are found through the boundary conditions (9) and (10), where h is the height of the considered layer (see Fig. 3).

$$H = \frac{I_{k-1}}{W_{sk}} \;\;;\;\; r = 0 \tag{9}$$

$$H = \frac{I_k}{W_{sk}} \;\;;\;\; r = h \tag{10}$$

The current density in the k-th layer is finally obtained as in (11), whereas the associated losses are finally determined as in (12). In (12), lck is the length of the k-th conductor in the slot region, while vol is its volume.

$$J_k = \\ -\frac{I_k\left(\frac{1+j}{\eta}\right)\cosh\left(\left(\frac{1+j}{\eta}\right)r\right) - I_{k-1}\left(\frac{1+j}{\eta}\right)\cosh\left(\left(\frac{1+j}{\eta}\right)h - \left(\frac{1+j}{\eta}\right)r\right)}{w_{sk}\sinh\left(\left(\frac{1+j}{\eta}\right)h\right)} \tag{11}$$

$$P_k = \iiint_0^{vol}\frac{J_k{}^2}{\sigma}\,dv = \;l_{ck}\,W_{ck}\int_0^h \frac{J_k{}^2}{\sigma}dr \tag{12}$$

B .Slot Region Model

In the end-winding region, the model described above cannot be directly used since the ferromagnetic material surrounding the conductors is no longer present and the geometry of the end-windings is rather complex. However, since the end-windings are basically surrounded by air, the magnetic field magnitude is much lower than the slot region. It becomes then reasonable to neglect the proximity effect [23], meaning that the only contribution to AC losses is due to the skin effect. As a first approximation, the skin effect can be considered invariant along the direction of the conductor length, thus leading to tackle the loss determination problem as a 1D one also in the end-winding region. Equation (13) is then used for determining the skin effect resistance Rskin [24], which depends on the parameter ξ the expression of which is provided in (14).

$$R_{skin} = \frac{R_{DC}}{2}\;\xi\;\frac{sinh(\xi)+sin\,(\xi)}{cosh(\xi)-cos\,(\xi)} \tag{13}$$

$$\xi = \frac{\sqrt{\pi}}{2}\,\frac{1}{\delta}\sqrt{\frac{W_{ck}\;h_c}{\pi}} \tag{14}$$

IV. FE Model

As per the analytical approach, FE models of both slot and end-winding regions are developed to evaluate the AC losses using MagNet® from Simcenter. For both regions, the solution mesh is defined according to a detailed sensitivity analysis aimed at finding the best trade-off between accuracy and computational effort. Time harmonic simulations are used for the sake of resolution speed and consistency with the sinusoidal supply assumption. According to the [25] only the stator model is needed to reduce the computational effort without losing accuracy in estimating the AC losses, being the latter mainly dependant on the slot flux leakage [20].

A .Slot Region Model

Contrarily to the analytical approach, for the slot region the FE models consist of 2 poles being analyzed for any of the 4 configurations introduced in Section II. Only one phase and only the stator is modelled, as shown in Fig. 4 for one of the considered layouts, i.e. the case with q=2 and k=4.

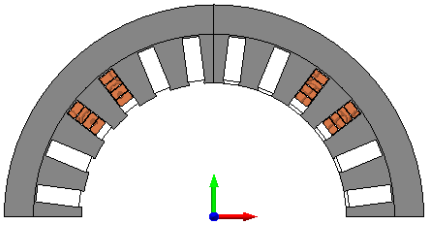

Fig. 4. FE slot region model for the case study with q=2 and k=4.

B .End Winding Region

The estimation of AC losses in hairpin windings including the end-windings is an inherently 3D problem. Also, the end regions of hairpin windings are rather complex and only a 3D analysis would be fully accurate. However, a 3D model would be very consuming in terms of both modeling and simulation times. To enable an 2D analysis, first of all the proximity effect is neglected and only the skin effect is taken into account, consistently to the analytical approach discussed in Section III. To simplistically evaluate the influence of the end-winding geometries, two conductors with different shapes are considered, as reported in Fig. 5. The two conductors have identical cross sections and lengths, but the first one is obtained through axial extrusion (see Fig. 5a), whereas the second one is extruded angularly (see Fig. 5b). Apart from the major bends typical of hairpin windings, the conductor shown in Fig. 5b reproduces a shape close approximation to the ones that can really be found in this region. This conductor is modelled through a 3D FEA, whereas the one shown in Fig. 5a is studied as a 2D problem. The FE evaluations for both conductors' shapes are carried out at 1000 Hz to enhance the high frequency effects. The comparison is shown in Table IV and highlights a 1.5% mismatch between the results in terms of losses. In Table IV, the number of mesh elements and the solution times are also reported to emphasize and justify the use of the 2D models for the analysis of the end-winding regions.

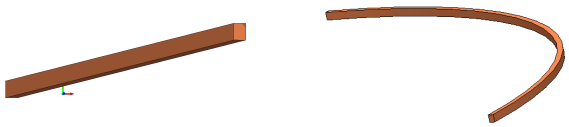

a) b)

Fig. 5. End Winding Region Models: a) Axially-extruded conductor (2D analysis) and b) Angularly-extruded conductor (3D analysis).

Table IV : Comparison AC Losses at 1kHz between 2D and 3D End Winding Models

Model	Losses [mW]	Mesh Elements (units)	Computational Time (sec)
2D	5.15	226	6
3D	5.23	711358	67

Considering the above and passing to the analysis of the study cases at hand, it is worth mentioning that a full 3D CAD model is usually available for a hairpin winding design ready to be manufactured. Hence, it would be straightforward to determine cross sections and lengths of all conductors to use in the simplified 2D FE models. However, since motorettes are manually built to prove the concepts proposed in this article, a full 3D CAD model is not available. Therefore, to estimate the end-winding length for the FE evaluations, first the overall DC resistance $R_{DCmeasured}$ is measured with an impedance analyzer and then, knowing the winding characteristics in the slot region, it becomes possible to extract the 2D resistance R_{DC2D} and the end-winding resistance and length R_{end} and L_{end}. To such purposes, (14) and (15) are used, where σ_{Cu} is the copper conductivity and A_{Cu} is the conductor cross section

$$R_{end} = \left(R_{DC_{measured}} - R_{DC_{2D}}\right) \quad (14)$$

$$L_{end} = R_{end}\ \sigma_{cu}\ A_{cu} \quad (15)$$

In Table V, the end-winding lengths calculated in this way are reported for each investigated case study. Finally, using such lengths, the simplified models shown in Fig. 6 are built to estimate the AC losses in the end-winding region of each considered winding layout.

Table V : End Winding Lengths

Winding Layout	End Winding Length [mm]
q=2 and k=4	396
q=4 and k=4	306
q=4 and k=4 Segmented	172
q=4 and k=8	13.4

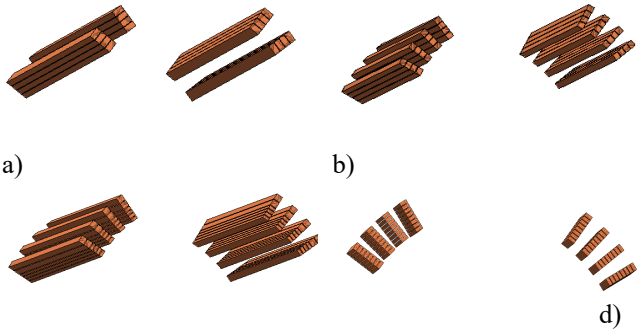

a) b) c) d)

Fig. 6. End winding region model: a) q=2 and k=4; b) q=4 and k=4; c) q=4 and k=4 segmented; d) q=4 and k=8.

V. Comparison between Analytical and FE Model Results

In this section the results obtained with the analytical and FE models described above are presented and compared. These results aim to highlight the accuracy of the analytical model and the importance of including the end-winding effects in the evaluation of the overall AC losses.

A. *Slot Region Model: Analytical vs FE results*

The results obtained from the developed slot region analytical and FE models are compared in Fig. 7, which shows the trend of the parameter K_{AC} (defined in (1)) vs. frequency. The machine electrical frequency at the maximum speed of

12000rpm is equal to 400Hz. However, the analysis is carried out for a frequency range up to 1200 Hz for a better understanding of the losses behaviour of the studied topologies and for potential applications at higher speeds and/or frequencies.. For the sake of clarity, the results relative to the four study cases have been split in Figures 7a and 7b. The match is very positive for all the conventional winding schemes, with a maximum error lower than 3% over the whole frequency range analyzed. Regarding the segmented layout, the error becomes ≈50% at 1200 *Hz* (see Fig. 7b), since the developed model does not take into account the updated boundary conditions resulting from such an unconventional arrangement [18]. On the other hand, both the analytical and FE results prove the perceived benefits of the segmented layout, with a significant loss reduction achieved compared to the conventional *q=4, k=4* configuration.

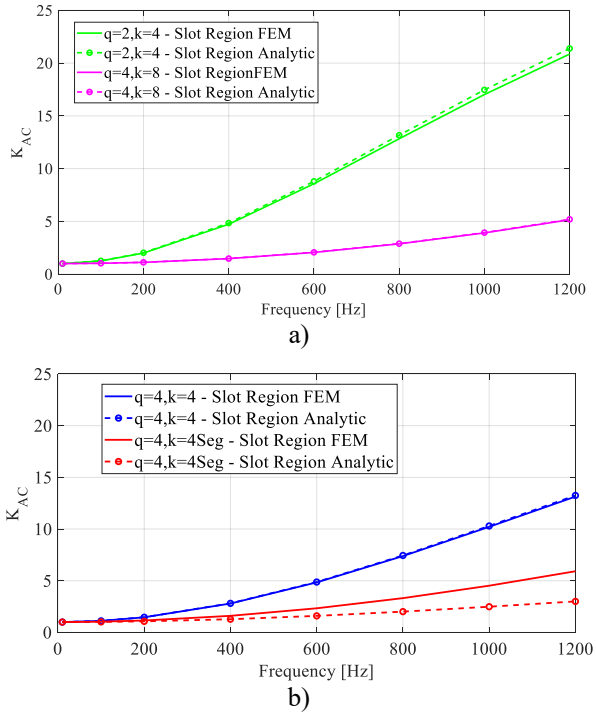

Fig. 7. Slot region models: analytical vs. FE results -a) q=2, k=4 and q=4, k=8; b) q=4, k=4 and q=4, k=4 segmented.

B. *Complete Analytical Model vs. Complete FE Model*

To evaluate the effects of the end winding regions on AC losses, the FE results shown in the section III(labelled as "Slot Region FEM") are compared against the complete FE model (labelled as "Complete FEM"), which includes both the contributions from the slot and end winding regions. The discrepancies can be very high, thus proving the need of an accurate end winding region model. The last comparison of this sensitivity study is carried out between analytical and FE models, when both include the overall effects (slot and end-winding regions) into account. The results are reported in Fig. 8, where the segmented hairpin is not reported as the discrepancy would be excessive due to the reasons given in Section V.A. It can be noticed that the analytical model is not as accurate as in the slot region. For the study cases q=4 with k=4, q=4 with k=8 and q=2 with k=4 the maximum errors are 28%, 15% and 17%, respectively.

Despite these discrepancies, it is worth underlying again the need of including the 3D effects also in the analytical model. In fact, this is faster than the FE evaluations and this can lead designers and researchers to prefer the analytical approach in some specific cases (e,g. when long optimization processes are used), yet accepting the inherent limitations and inaccuracies.

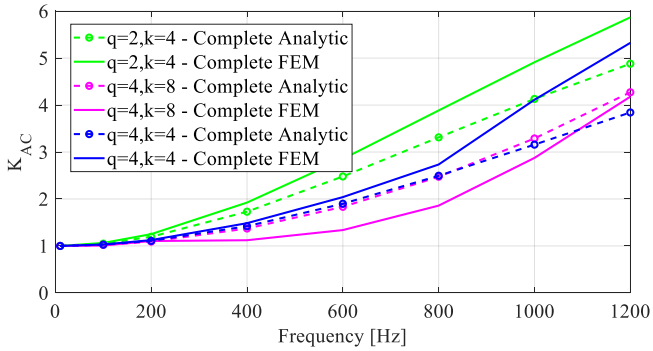

Fig. 8. Complete analytical model vs. complete FE model: comparison of results relative to the investigated conventional arrangements.

VI. THERMAL ANALYSIS

The loss reduction achieved by the segmented hairpin winding would lead to a temperature reduction which could lead either to increase the power rating of the electrical machine or to operate it at a lower temperature in order to extend the insulation lifetime. For the sake of completeness, a thermal analysis via Simcenter MAGNET Thermal is performed on the segmented hairpin and its conventional version. The environmental condition boundaries are set in the surfaces in contact with the ambient air, imposing an environmental temperature of 20°C and a convective heat transfer coefficient of 20W/(m^2 °C) according to [26]. Coupled simulations are carried out using the electromagnetic field simulation software Simcenter MagNet and the thermal tool MAGNET Thermal. First, 2D time harmonic simulations are made to evaluate the losses, and then these are automatically acquired by the thermal software and used as heat sources for the 2D static thermal simulations. A significant operating point at a frequency equal to 1kHz is chosen for the comparison, with the current set at 40A to achieve reasonable temperature levels. Figure 9 shows the temperature distribution for the standard solution (Fig. 9a) and for the proposed concept (Fig. 9b).

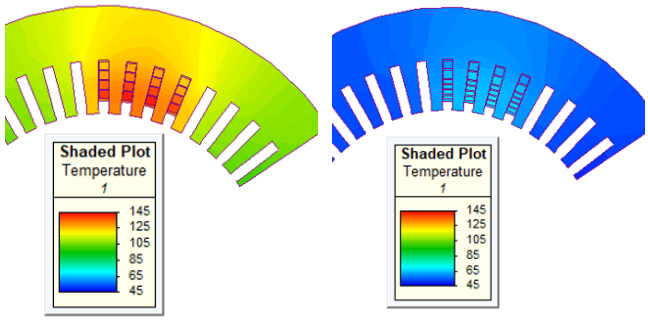

a) b)

Fig.9. Temperature distribution for a) the conventional winding topology and b) the proposed winding topology.

With the proposed solution the peak temperature registered in the conductors is 67.8 °C, whereas with the standard solution the peak temperature is 141.9 °C. These values are justified by the significantly different values of copper losses produced with the conventional and the segmented configurations, being respectively equal to 119W and 52.9W. The ratio

between losses is consistent with what is reported in Fig. 7.b where, at 1kHz, for the conventional hairpin winding KAC is about twice that of the segmented layout.

VII. Experimental Results

Aiming at demonstrating the proposed segmented concept as a means to reduce AC losses in hairpin windings, as well as to prove the methodologies presented in the previous section, four motorettes (i.e. stator portions corresponding to one pole pair) are built according to the dimensions provided in Tables II and III. As mentioned in Section IV.B, these motorettes are manually wound for the sake of simplicity, i.e. to minimize costs, resulting in oversized end-windings as observed in the figure. The motorettes are shown in Fig. 10 and are representative of the four study cases investigated in this work. Therefore, one of these implements the segmented hairpin winding concept, i.e. the one labelled as "q=4, k=4 Seg" in Fig. 10. For the sake of consistency with the sinusoidal supply assumptions used in both analytical and FE evaluations, the signal feeding the motorettes is first produced by a SiC Voltage Pulse generator with 60 *kHz* switching frequency and, then, filtered by a low pass LC filter with a cutoff frequency at 2 *kHz* to obtain an output signal as close as possible to a pure sinusoidal waveform. The power loss is measured by a precision power analyzer (PPA 5530) and an oscilloscope is used to double check the losses value and the signal waveforms. All measurements are taken at the same temperature ($20\,°C$). and the winding temperatures are monitored with a thermal camera during testing. The whole test setup is shown in Fig. 11a, whereas the relevant circuital schematic is illustrated in Fig. 11b.

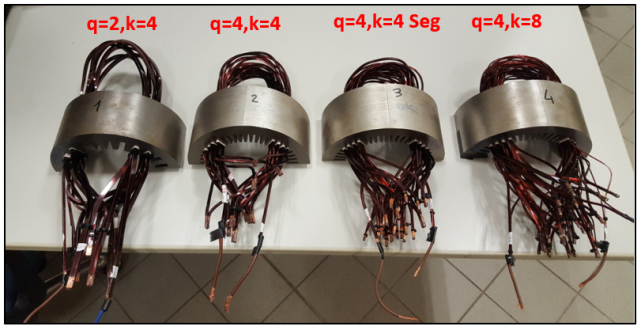

Fig. 10. Built motorettes.

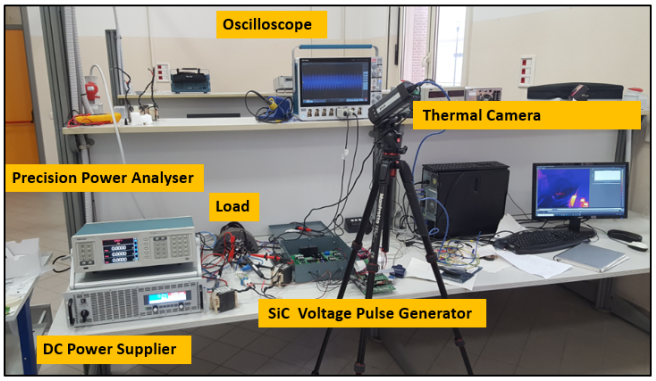

a)

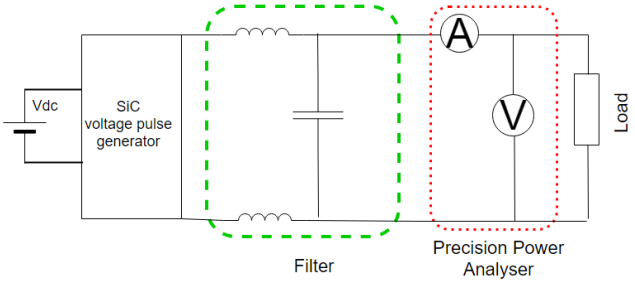

b)

Fig. 11. a) Experimental setup and b) corresponding circuital schematic.

The experimental tests are performed ranging from 0 *Hz* to 1200 *Hz* and the relevant results are compared in terms of K_{AC} against the complete FE simulation results. This comparative exercise is reported in Fig. 12, where an excellent match between FE and experimental results is achieved in the whole frequency range considered. The maximum error is less than 15% and this could be justified by the additional resistance introduced by the welded connections.

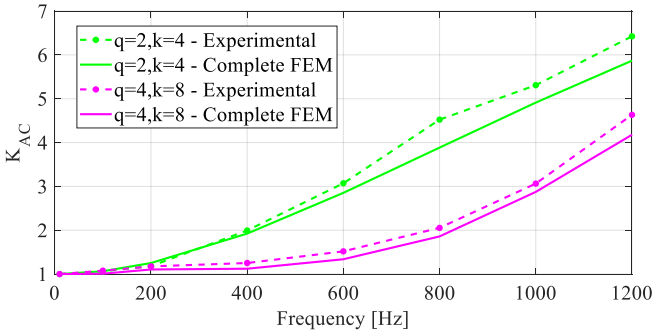

a)

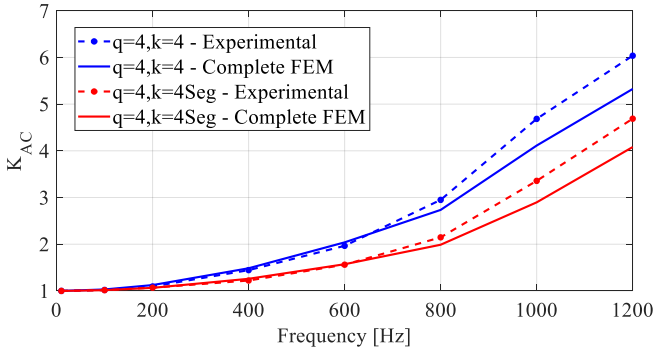

b)

Fig. 12. Comparison between FE and experimental results: a) q=2, k=4 and q=4, k=8; b) q=4, k=4 and q=4, k=4 segmented.

Apart from the match accuracy between FE and experimental results, the main achievement here is the proof of the effectiveness of the segmented hairpin concept. Compared to the conventional q=4, k=4 layout, its modified segmented version, i.e. q=4, k=4 segmented, achieves an experimental loss reduction by more than 20% starting from 600 *Hz*, with a peak reduction of 28% registered at 1000 *Hz*. It is worth mentioning that, as done for the analytical and FE evaluations, the same magneto-motive force is used to feed the hairpin layouts to make the comparison fully fair.

Having proven the effectiveness of the proposed technique, the last step is to demonstrate that the segmented hairpin windings can compete against random windings envisioned for the same application. This is the focus of the next section.

VIII. Comparison Between Hairpin and Random Experimental Results

For the same application (see Section II), motorettes with trapezoidal slots hosting a random winding with round conductors are built and tested in order to identify the trend of the parameter K_{AC} vs. frequency. The full analysis and experimental campaign are detailed in [22], where different winding topologies were proposed with the goal of achieving an optimal solution for reduced copper losses. The built motorettes are shown in Fig. 13, with two configurations being realized: $q=2$ and $q=4$. The winding details are summarized in Table VI.

In [22], it was found that the AC losses are significantly dependent on the position of the various strands, especially for high frequency operating points. Hence, in this work, where the results have to be compared against those relative to the hairpin motorettes, the trend of K_{AC} is plotted considering a mean value μ_{ESM} and a standard deviation σ_{ESM} found out leveraging on the experimental statistical method [22].

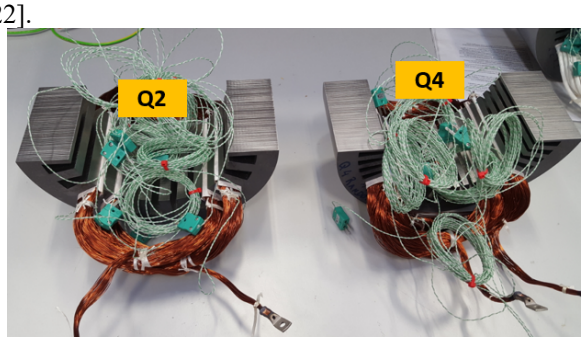

Fig. 13. Motorettes with random windings.

Table VI : Winding Details

Parameter	Value	
	Q2	Q4
Strands in hand	32	32
Turns per phase	16	8
Strand (copper) diameter (mm)	0.56	0.56
Slot Filling Factor (%)	44	44

Fig. 14 shows the experimental comparison between hairpin and random windings in terms of K_{AC} vs. frequency, up to 1 *kHz*. For the random winding, the minimum and maximum K_{AC} values that give the 66% probability of having a value inside the range $\mu_{ESM} \mp \sigma_{ESM}$ are considered. It can be noticed that the hairpin solutions perform better than the random ones in the low frequency range. This is due to the higher slot fill factor and the ensuing lower DC resistance. Most importantly, Fig. 14 highlights that the 2 hairpin solutions q=4, k=8 and q=4, k=4 segmented achieve lower losses than the 66% of the possible solutions that can happen with random windings up to ≈900 *Hz*. These results, besides proving that some hairpin layouts (including the proposed segmented one) can present lower losses than random windings even at high frequency operations, also demonstrate that the segmented layout presents similar performance to the 8-layer hairpin configuration, albeit with a reduced number of layers per slot, thus potentially leading to a simplification of the manufacturing process.

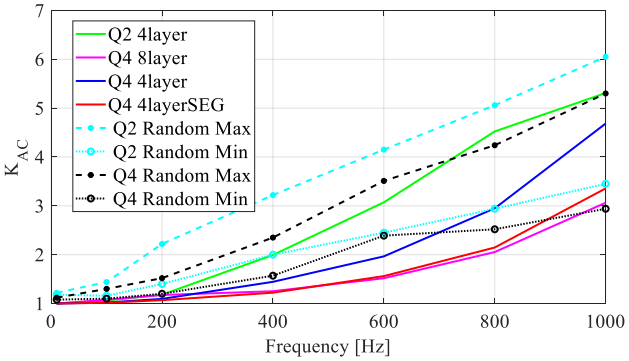

Fig. 14. Experimental results: random vs. hairpin windings.

IX. Conclusions

In this work, an improved hairpin winding topology was proposed to reduce ohmic losses at high frequency operations. This concept, named as segmented hairpin, consists of splitting one or more slot conductors in two or more sub-conductors, similarly to the "strand" concept usually implemented in random windings. In this paper, it was decided to split two conductors in two sub-conductors, as this was deemed to be the optimal solution in terms of loss reduction and minimization of the manufacturing complexities.

The losses produced at various frequency operations within the proposed segmented hairpin winding were assessed against conventional hairpin and random solutions. Analytical and finite element models were used to such purposes, taking into account both slot and end-winding regions. A simplified 2D finite element model was implemented to predict losses in the end-windings, thus avoiding the need of building an accurate but very computationally-expensive 3D model. The relevant findings proved that the AC end-winding losses can be significant is some cases, whereas they are regularly overlooked in previous literature.

In terms of loss reduction, promising analytical and finite element results were obtained for the proposed segmented concept. These perceived benefits were then validated by building and testing stator motorettes featuring various winding arrangements. Compared to conventional hairpin layouts, the segmented hairpin solution achieved a loss reduction always higher than 20% starting from ≈600 Hz, reaching a peak reduction of 28% at 1 kHz, thus proving its potential.

Finally, a comparison between random and hairpin windings designed for the same traction application was performed. Both conventional and segmented hairpin layouts provided lower losses than random windings at low frequency, as expected. Additionally and importantly, the proposed segmented hairpin solution achieved loss values similar to random windings up to 900 Hz, thus proving its competitiveness for a broader range of operational frequencies.

ACKNOWLEDGEMENT

This project has received funding from the Clean Sky 2 Joint Undertaking under the European Union's Horizon 2020 research and innovation programme under grant agreement No. 865354

X. REFERENCES

[1] Y. -H. Jung, M. -R. Park, K. -O. Kim, J. -W. Chin, J. -P. Hong and M. -S. Lim, "Design of High-Speed Multilayer IPMSM Using Ferrite PM for EV Traction Considering Mechanical and Electrical Characteristics," in IEEE Transactions on Industry Applications, vol. 57, no. 1, pp. 327-339, Jan.-Feb. 2021.

[2] V. Madonna, P. Giangrande, J. Harikumaran, G. Buticchi and M. Galea, "System Level Reliability Assessment of Short Duty Electric Drives for Aerospace," in IEEE Transactions on Transportation Electrification.doi: 10.1109/TTE.2021.3053147

[3] E. Bostanci, M. Moallem, A. Parsapour and B. Fahimi, "Opportunities and Challenges of Switched Reluctance Motor Drives for Electric Propulsion: A Comparative Study," in IEEE Transactions on Transportation Electrification, vol. 3, no. 1, pp. 58-75, March 2017.

[4] M. Mezzarobba et al., "Design, Prototyping and Testing of a Rotating Electrical Machine With Linear Geometry for Shipboard Applications," in IEEE Access, vol. 8, pp. 122884-122897, 2020.

[5] Hyung-Woo Lee, Tae-Hyung Kim and M. Ehsani, "Practical control for improving power density and efficiency of the BLDC generator," in IEEE Transactions on Power Electronics, vol. 20, no. 1, pp. 192-199, Jan. 2005.

[6] S. Baek, G. Kim and H. Shin, "Maximization of Efficiency of IPMSM by Quasi-Newton Method," 2018 21st International Conference on Electrical Machines and Systems (ICEMS), Jeju, 2018,pp.472-475.doi: 10.23919/ICEMS.2018.8549065.

[7] P. Giangrande, V. Madonna, S. Nuzzo and M. Galea, "Moving Toward a Reliability-Oriented Design Approach of Low-Voltage Electrical Machines by Including Insulation Thermal Aging Considerations," in IEEE Transactions on Transportation Electrification, vol. 6, no. 1, pp. 16-27, March 2020.

[8] Cui Shu-mei, Huang Wen-xiang and Zhang Qian-fan, "Research on power density improvement design of an HEV using induction machine based electrical variable transmission," 2008 IEEE Vehicle Power and Propulsion Conference, Harbin, China, 2008, pp. 1-4.

[9] Y. Wang, T. Balachandran, Y. Hoole, Y. Yin and K. S. Haran, "Partial Discharge Investigation of Form-Wound Electric Machine Winding for Electric Aircraft Propulsion," in IEEE Transactions on Transportation Electrification, vol. 6, no. 4, pp. 1638-1647, Dec. 2020.

[10] M. Pastura et al., "Partial Discharges in Electrical Machines for the More Electric Aircraft—Part I: A Comprehensive Modeling Tool for the Characterization of Electric Drives Based on Fast Switching Semiconductors," in IEEE Access, vol. 9, pp. 27109-27121, 2021, doi: 10.1109/ACCESS.2021.3058083.

[11] C. Du-Bar, A. Mann, O. Wallmark and M. Werke, "Comparison of Performance and Manufacturing Aspects of an Insert Winding and a Hairpin Winding for an Automotive Machine Application," 2018 8th International Electric Drives Production Conference (EDPC), Schweinfurt, Germany, 2018, pp. 1-8.

[12] G. Berardi, S. Nategh, N. Bianchi and Y. Thioliere, "A Comparison Between Random and Hairpin Winding in E-mobility Applications," IECON 2020 The 46th Annual Conference of the IEEE Industrial Electronics Society, Singapore, 2020, pp. 815-820.

[13] N. Bianchi and G. Berardi, "Analytical Approach to Design Hairpin Windings in High Performance Electric Vehicle Motors," 2018 IEEE Energy Conversion Congress and Exposition (ECCE), Portland, OR, 2018, pp. 4398-4405.

[14] W. Zhang and T. M. Jahns, "Analytical 2-D slot model for predicting AC losses in bar-wound machine windings due to armature reaction," 2014 IEEE Transportation Electrification Conference and Expo (ITEC), Dearborn, MI, 2014, pp. 1-6.

[15] E. Preci et al., “Hairpin Windings: Sensitivity Analysis and Guidelines to Reduce AC losses”, proceeding on 2021 IEEE Workshop on Electrical Machines Design, Control and Diagnosis (WEMDCD), Modena, Italy, 2021

[16] C. Du-Bar, A. Mann, O. Wallmark and M. Werke, "Comparison of Performance and Manufacturing Aspects of an Insert Winding and a Hairpin Winding for an Automotive Machine Application," 2018 8th International Electric Drives Production Conference (EDPC), Schweinfurt, Germany, 2018, pp. 1-8.

[17] M. S. Islam, I. Husain, A. Ahmed and A. Sathyan, "Asymmetric Bar Winding for High-Speed Traction Electric Machines," in IEEE Transactions on Transportation Electrification, vol. 6, no. 1, pp. 3-15, March 2020.

[18] A. Arzillo et al., "An Analytical Approach for the Design of Innovative Hairpin Winding Layouts," 2020 International Conference on Electrical Machines (ICEM), Gothenburg, Sweden, 2020, pp. 1534-1539.

[19] E. Schmidt and C. Grabner, "Application of a weak coupling algorithm in the electromagnetic-mechanical finite-element analysis for Roebel bars of large synchronous machines," in IEEE Transactions on Magnetics, vol. 41, no. 5, pp. 1896-1899, May 2005. doi: 10.1109/TMAG.2005.846256

[20] E. Preci et al., "Rectangular and Random Conductors: AC Losses Evaluations and Manufacturing Considerations," IECON 2020 The 46th Annual Conference of the IEEE Industrial Electronics Society, Singapore, 2020, pp. 1076-1081.

[21] E. Preci et al., "Experimental Statistical Method Predicting AC Losses on Random Windings and PWM Effect Evaluation," in IEEE TransactionsonEnergyConversion.doi: 10.1109/TEC.2020.3040265

[22] http://www.automea.unimore.it/

[23] H. Hämäläinen, J. Pyrhönen and J. Nerg, "AC Resistance Factor in One-Layer Form-Wound Winding Used in Rotating Electrical Machines," in IEEE Transactions on Magnetics, vol. 49, no. 6, pp. 2967-2973, June 201

[24] J. A. Ferreira, "Improved analytical modeling of conductive losses in magnetic components," in IEEE Transactions on Power Electronics, vol. 9, no. 1, pp. 127-131, Jan. 1994.
[25] M. van der Geest, H. Polinder, J. A. Ferreira and D. Zeilstra, "Stator winding proximity loss reduction techniques in high speed electrical machines," 2013 International Electric Machines & Drives Conference, Chicago, IL, USA, 2013, pp. 340-346.
[26] J. P. Holman, Heat Transfer. New York: McGraw-Hill, 1997

XI. BIOGRAPHIES

Eraldo Preci (S'17-M'18) received the B.Sc. and M.Sc. (Hons.) degrees in Electrical Engineering from the University of Pisa, Pisa, Italy, in 2010 and 2013, respectively. From 2014 to 2017 he has worked for Intertek Italia as a consultant for General Electric Turbomachinery, Italy. Since 2018 he is pursuing an exchange Ph.D. degree with the Power Electronics, Machines and Control (PEMC) Group, University of Nottingham, between the two campuses based in Nottingham, U.K and Ningbo , China. His main research interests are the modelling, analysis and multiphysics optimization of electrical machines and drive. Mr. Preci received the qualification of Italian Chartered Engineer in 2015.

Stefano Nuzzo (S'17-M'18) received the B.Sc. and M.Sc. degrees in Electrical Engineering from the University of Pisa, Pisa, Italy, in 2011 and 2014, respectively. He received his Ph.D. degree in Electrical Engineering in 2018 from the University of Nottingham, Nottingham, U.K, where he worked also as a Research Fellow within the Power Electronics, Machines and Control (PEMC) Group. Since January 2019, he works within the Department of Engineering "Enzo Ferrari" at University of Modena and Reggio, Modena, Italy, where he is a Lecturer in Electrical Machines ad Drives. His research interests are the analysis, modelling and optimizations of electrical machines intendend for power generations, industrial and transport applications. He is involved in a number of projects related to the more electric aircraft initiative and associated fields. Dr. Nuzzo is a Member of the IEEE Industrial Electronics Society (IES) and the IEEE Industry Applications Society (IAS). He constantly serves the scientific community as a reviewer for several journals and conferences.

Giorgio Valente received the master degree (Hons.) in electrical engineering from the University of Padova, Italy, in 2014, and the Ph.D. degree inelectrical machines design and control from the University of Nottingham, U.K., in 2018. He then worked for two years as a Research Fellow with the Power Electronics, Machines and Control Group, University of Nottingham, U.K. He is now working as Electric Machine Design and Development Engineer in Romax Technology Ltd, Nottingham, U.K. His research interests include bearingless machines design and control, high speed machines, traction machines, and multiphysics-based optimization of electrical machine

David Gerada received the Ph.D. degree in high-speed electrical machines from University of Nottingham, Nottingham, U.K., in 2012. From 2007 to 2016, he was with the R&D Department at Cummins, Stamford, U.K., first as an Electromagnetic Design Engineer (2007– 2012), and then as a Senior Electromagnetic Design Engineer and Innovation Leader (2012– 2016). At Cummins, he pioneered the design and development of high-speed electrical machines, transforming a challenging technology into a reliable one suitable for the transportation market, while establishing industry-wide-used metrics for such machinery. In 2016, he joined the University of Nottingham where he is currently a Principal Research Fellow, responsible for developing state-of-the-art electrical machines for future transportation which push existing technology boundaries, while propelling the new technologies to higher technology readiness levels. Dr. Gerada is a Chartered Engineer in the U.K. and a member of the Institution of Engineering and Technology

Davide Barater (M'14-S'21) received the Master's degree in Electronic Engineering in 2009 and the Ph.D. degree in Information Technology in 2014 from the University of Parma Italy. He was an honorary scholar at the University of Nottingham, U.K., during 2012, and a visiting researcher at the University of Kiel, DE in 2015.

He is currently Associate Professor at Department of Engineering "Enzo Ferrari", University of Modena and Reggio Emilia, Italy. His research area is focused on power electronics for e-mobility and motor drives.
He is the Coordinator of two European Project AUTO-MEA that aims to develop electrical motors and drives for next generation of electrical mobility. In particular, novel solutions for windings structures and cooling systems for improved power density, efficiency and increased frequency operation. https://www.automea.unimore.it
He is Associate Editor of IEEE Transactions on Industry Applications and author or co-author of more than 70 international papers.

Michele Degano (M'15) received his Master's degree in Electrical Engineering from the University of Trieste, Italy, in 2011, and his Ph.D. degree in Industrial Engineering from the University of Padova, Italy, in 2015. Between 2014 and 2016, he was a post-doctoral researcher at The University of Nottingham, UK, where he joined the Power Electronics, Machines and Control (PEMC) Research Group. In 2016 he was appointed Assistant Professor in Advanced Electrical Machines, at The University of Nottingham, UK. He was promoted Associate Professor in 2020. His main research focuses on electrical machines and drives for industrial,

automotive, railway and aerospace applications, ranging from small to large power. He is currently the PEMC Director of Industrial Liaison leading research projects for the development of hybrid electric aerospace platforms and electric transports

Giampaolo Buticchi received the Master degree in Electronic Engineering in 2009 and the Ph.D degree in Information Technologies in 2013 from the University of Parma, Italy .In 2012 he was visiting researcher at The University of Nottingham, UK. Between 2014 and 2017, he was a post-doctoral researcher, and Guest Professor at the University of Kiel, Germany. During his stay in Germany, he was awarded with the Von Humboldt Post-doctoral Fellowship to carry out research related to fault tolerant topologies of smart transformers.
In 2017 he was appointed as Associate Professor in Electrical Engineering at The University of Nottingham Ningbo China and as Head of Power Electronics of the Nottingham Electrification Center. He was promoted to Professor in 2020.
His research focuses on power electronics for renewable energy systems, smart transformer fed micro-grids and dc grids for the More Electric Aircraft. Dr. Buticchi is one of the advocates for DC distribution systems and multi-port power electronics onboard the future aircraft.
He is author/co-author of more than 210 scientific papers, an Associate Editor of the IEEE Transactions on Industrial Electronics, the IEEE Transactions on Transportation Electrification and the IEEE Open Journal of the Industrial Electronics Society. He is currently the Chair of the IEEE-IES Technical Committee on Renewable Energy Systems and the IES Energy Cluster Delegate

Chris Gerada (SM'12) is an Associate Pro-Vice-Chancellor for Industrial Strategy and Impact and Professor of Electrical Machines. His principal research interest lies in electromagnetic energy conversion in electrical machines and drives, focusing mainly on transport electrification. He has secured over £20M of funding through major industrial, European and UK grants and authored more than 350 referred publications. He received the Ph.D. degree in numerical modelling of electrical machines from The University of Nottingham, Nottingham, U.K., in 2005. He subsequently worked as a Researcher with The University of Nottingham on high-performance electrical drives and on the design and modelling of electromagnetic actuators for aerospace applications. In 2008, he was appointed as a Lecturer in electrical machines; in 2011, as an Associate Professor; and in 2013, as a Professor at The University of Nottingham. He was awarded a Research Chair from the Royal Academy of Engineering in 2013. Prof. Gerada served as an Associate Editor for the IEEE Transactions on Industry Applications and is the past Chair of the IEEE IES Electrical Machines Committee